



SPE-15862-GF

Assessment of Seafloor Conditions and Sediment Deposition using Machine Learning Classifiers

Addison Richter, Cody Thayer, and Eugene Reveals

Copyright 2021, Society of Petroleum Engineers International

This paper was prepared for presentation at the Society of Petroleum Engineers International Conference held in New Orleans, Louisiana, USA, Sept 2021.

This paper was selected for presentation by an SPE program committee following review of information contained in an abstract submitted by the author(s). Contents of the paper have not been reviewed by the SPE Conference and are subject to correction by the author(s). The material does not necessarily reflect any position of the SPE Conference, its officers, or members. Electronic reproduction, distribution, or storage of any part of this paper without the written consent of the SPE Conference is prohibited. Permission to reproduce in print is restricted to an abstract of not more than 300 words; illustrations may not be copied. The abstract must contain conspicuous acknowledgment of SPE copyright.

Abstract

Objectives/Scope: Sediment profile imaging (SPI) technology characterizes *in situ* physical, geochemical, and biological seafloor features. SPI was required by Mexico's Agency for Safety, Energy, and Environment in 2017 for environmental baseline surveys (EBS) of oil lease blocks in the southern Gulf of Mexico. Because of its ability to provide information on benthic community health and the distribution of very thin (down to the centimeter scale) layers of deposited materials, SPI technology is highly effective for mapping drill cuttings or drilling muds released around wellheads during exploration or production and documenting their ecological impacts. SPI technology has not been widely used in the oil and gas industry for EBS or other monitoring activities. A primary objective of this work is to improve the transparency and consistency of the SPI data generation and data management process.

Methods, Procedures, Process: The SPI camera works like an inverted periscope and obtains an undisturbed 21x15-cm cross-sectional image of the upper sediment column. The camera is internally powered and can be deployed rapidly from a standard winch in depths to 4,000 m. Many stations can be sampled in a single day by “pogo-sticking” across a survey area. Sediment grain size, penetration depth, surface boundary roughness, natural and anthropogenic depositional layers, depth of the oxidized surface sediment layer, maximum biogenic mixing depth, and infaunal successional stage can be directly measured at sea or immediately following the cruise. Final SPI data sets can be provided within a few weeks of the survey.

Results, Observations, Conclusions: Details on the features measured in SPI images and the underlying interpretive paradigms are presented. To standardize the SPI data generation process, Maxon Consulting has developed 1) a semiautomated image analysis platform, and 2) a SPI data-specific database architecture that allows both numerical and non-numerical metrics to be incorporated into a standard database structure. An integrated, software-based SPI analysis platform has been developed that imports image files and metadata and provides a graphical user interface. The software automatically stores the data, which can then be reviewed for quality assurance, plotted, statistically analyzed, and mapped or exported to other platforms (e.g., Esri ArcGIS©) for further evaluation. Image processing algorithms have been developed using a combination of open-source and commercially available software packages (e.g., MATLAB® and OpenCV) to automatically quantify key parameters.

Novel/Additive Information: SPI technology's underutilization in the oil and gas industry may be in part due to a lack of standardization in the measurement of basic features in SPI images. A primary objective of this work is to develop a streamlined, standardized, and transparent process for generating and managing SPI data.

Introduction

Sediment profile imaging (SPI) was developed in the 1970s to examine the *in situ* appearance of near-surface sediments (Rhoads and Cande 1971). This view of the top 20 cm, or so, of the sediment column in profile provides a unique view of physical, biological, and chemical sediment conditions. The approach was pioneered by research scientists interested in animal-sediment interactions, sedimentary structures and processes, and the interpretation of biogenic features in the geological record. Over the past five decades, this unique, seafloor photographic technology has been used to address a range of benthic research topics and applied aquatic environmental monitoring questions. Germano et al. (2011) provides a detailed account of the development of SPI technology, the underlying scientific principles, and its many applications.

Since the early 1990s, SPI has been used in environmental assessment studies for the offshore oil and gas industry (e.g., see Rumohr and Schomann 1992; CSA 2006; DBTWG 2011). SPI applications include: 1) baseline characterizations of the seafloor prior to project development; 2) monitoring potential impacts to benthic habitats during exploration and production; and 3) assessing the impacts of oil spills and sediment hydrocarbon contamination (Diaz et al. 1993), most notably as part of extensive seafloor surveys around the Macondo wellhead following the Deepwater Horizon spill (DBTWG 2011). Key advantages of SPI technology as an *in situ* sampling device are: 1) the relatively rapid and high-density spatial coverage that can be achieved; 2) the synoptic collection of geological, geochemical, and biological information; and 3) its effectiveness at detecting and mapping the distribution of thin (i.e., centimeter scale) anthropogenic deposits, such as drilling muds and cuttings. SPI surveys can also provide evidence of the physical disturbance and altered sedimentation/erosional patterns due to seabed mining operations, and around engineered seabed structures, such as pipelines and subsea equipment (Diaz et al. 2004; Germano & Associates 2010). In conjunction with traditional data sets, such as sediment chemistry and benthic infauna data, SPI can be a powerful complementary tool for evaluating sedimentological conditions and processes, and assessing the benthic ecological response of disturbance (Diaz et al. 2003; Valente et al. 1992).

Despite its proven track record as an effective benthic survey tool, SPI has been underutilized in the oil and gas industry. As noted above, although it has been used as an environmental monitoring tool in the oil and gas sector, until recently SPI technology has not been a mandatory element of the environmental baseline studies (EBS) required for oil field development. In 2017, SPI was included as a required element for EBS for oil lease blocks in the southern Gulf of Mexico by Mexico's Agency for Safety, Energy, and Environment (ASEA). SPI technology is also being used for environmental siting and monitoring studies associated with offshore renewable energy developments such as windfarms, and tidal and wave energy converters. Overall, this has resulted in an increased demand for SPI surveys in recent years.

Currently, there are only a handful of private-sector SPI technology providers worldwide and, as of February 2021, all are based in the U.S. or Europe.¹ Perhaps more significantly, the interpretation of the sedimentological and ecological significance of subtle variations in sediment color, texture, and patterns evident in SPI images can require an in-depth understanding of the benthic processes that create these patterns (Germano et al. 2011). Direct experience analyzing numerous (1,000s) of images may be needed to achieve consistent and accurate image analysis results and there are relatively few skilled SPI image analysts and little to no information exchange or data sharing among SPI practitioners due to the competitive business environment. In our opinion, this has led to a lack of standardization and transparency in the image analysis and SPI data generation process among SPI practitioners.

To address this issue, Maxon Consulting. (Maxon) SPI scientists and programmers have designed and prototyped a semiautomated computer image analysis platform (iSPI v0.1a) using state-of-the-art image processing and computer learning tools. The goal of this image analysis platform is to streamline and automate the generation, storage, and management of the data gleaned from the images to ensure that the SPI datasets are standardized, transparent, and can be readily shared with and reviewed by clients and regulators.

¹ U.S.-based companies that provide SPI image survey (including image analysis and reporting) include Maxon Consulting, Inspire Environmental, Newfields, and Diaz & Daughters; Europe-based firms include Aquafact, Ltd.

In this paper, we briefly describe how the SPI camera works, the key parameters measured from the images, and the underlying paradigms supporting the SPI data interpretation. We then describe the architecture of the image analysis platform, illustrate its success at automated image processing, and discuss the next steps in this platform's development.

SPI Image Collection

Ocean Imaging Systems (Pocasset, Massachusetts) is the main supplier of sediment profile camera systems. Their Model 3731-D Sediment Profiling System is a self-contained photographic system that takes high-resolution *in situ* digital images of the sediment-water interface (SWI) at water depths up to 4,000 m. The camera system features a Nikon D7100 digital camera set within a water-tight housing on top of a wedge-shaped prism. This prism assembly is mounted on a moveable carriage within a robust stainless steel frame. The frame is lowered to the seafloor on a winch wire, and the tension on the wire keeps the prism in its "up" position. When the frame lands on the seafloor and the winch wire goes slack, the camera prism descends into the sediment at a slow, controlled rate by the dampening action of a hydraulic piston to minimize disturbance of the SWI. On the prism's descent, a trigger is tripped that activates a time-delay circuit of variable length (operator-selected) to allow the camera to penetrate the seafloor before the image is taken. Figure 1 illustrates this deployment sequence. After the first replicate image is obtained at a target location, the camera is raised several meters off the bottom and a wiper blade mounted on the frame removes sediment adhering to the faceplate. The strobe recharges and the camera is ready to be lowered again for a second image or towed to the next target location. As shown in Figure 1, a plan view (PV) camera is often deployed with the SPI camera to obtain an image of the seabed immediately prior to and in front of the area where SPI image will be taken.

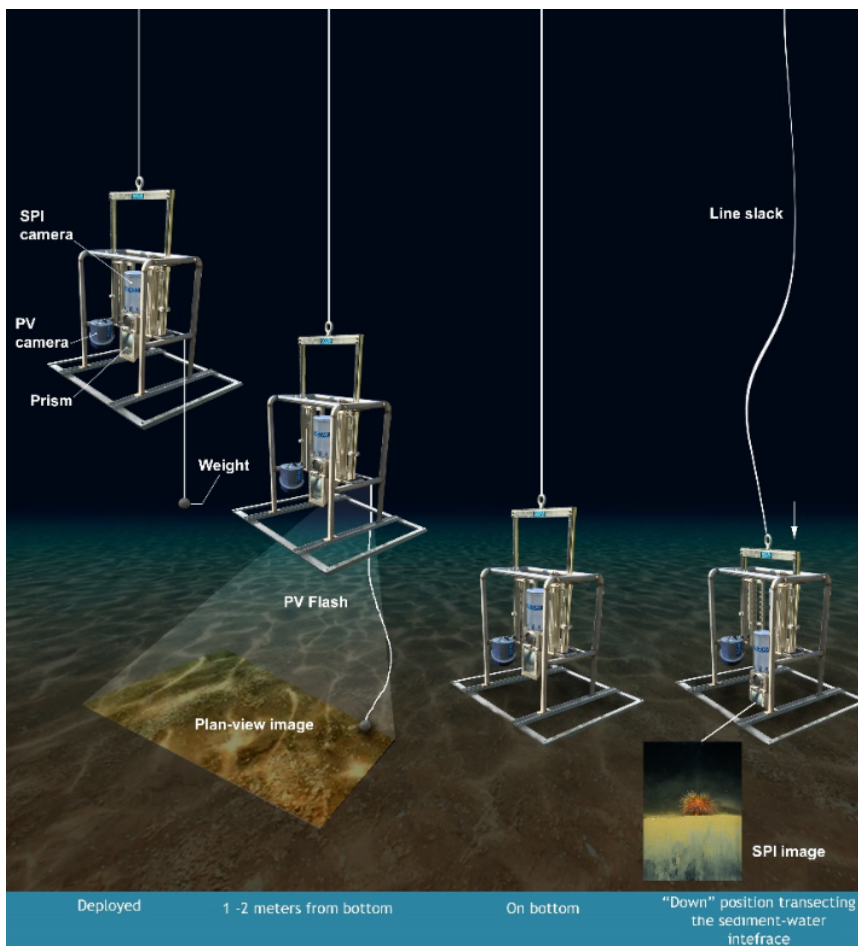


Figure 1. The SPI/PV camera deployment sequence.

The SPI camera prism has a Plexiglas® window at the front and a mirror on the bottom wedge at a 45° angle. The camera lens looks down at the mirror, which reflects the image of the sediment column against the window. The prism window and scale of the SPI image is approximately 15 cm wide by 22 cm high. The prism has an internal strobe mounted inside at the back of the wedge to provide illumination for the image; this chamber is filled with distilled water, so image quality is unaffected by near-bottom water turbidity and the resulting images give the viewer the same perspective as looking through the side of an aquarium filled with sediment (see inset in Figure 1).

SPI Image Analysis and Interpretation

There is an extensive body of literature on the interpretation of features observed and measured in SPI images (see Germano et al. 2011 and references therein). As a very general overview, the interpretation of physical features in SPI images is based on the measurements, and the inferences that can be made about sedimentary processes, from the textures, structures, strata, and bedforms imaged in the vertical profiles and mapped horizontally. The interpretation of geochemical features in SPI images is based on an understanding of redox chemistry with depth in the sediment column and the associated changes in sediment color (Fenchel 1969; Lyle 1983), as well as other indicators of sediment organic loading and oxygen levels (e.g., redox boundaries contrast, the presence of thiophilic bacterial mats at the SWI, and/or sedimentary methane at depth). The interpretation of biological features in SPI images is based on identification of the general types of organisms present coupled with an understanding of their life habitats, as well as the well-established paradigm first presented in Pearson and Rosenberg (1978) and adapted for the interpretation of animal-sediment structures in SPI images by in Rhoads and Boyer (1982) and Rhoads and Germano (1982, 1986) regarding the response of benthic communities to disturbance (Figure 2).

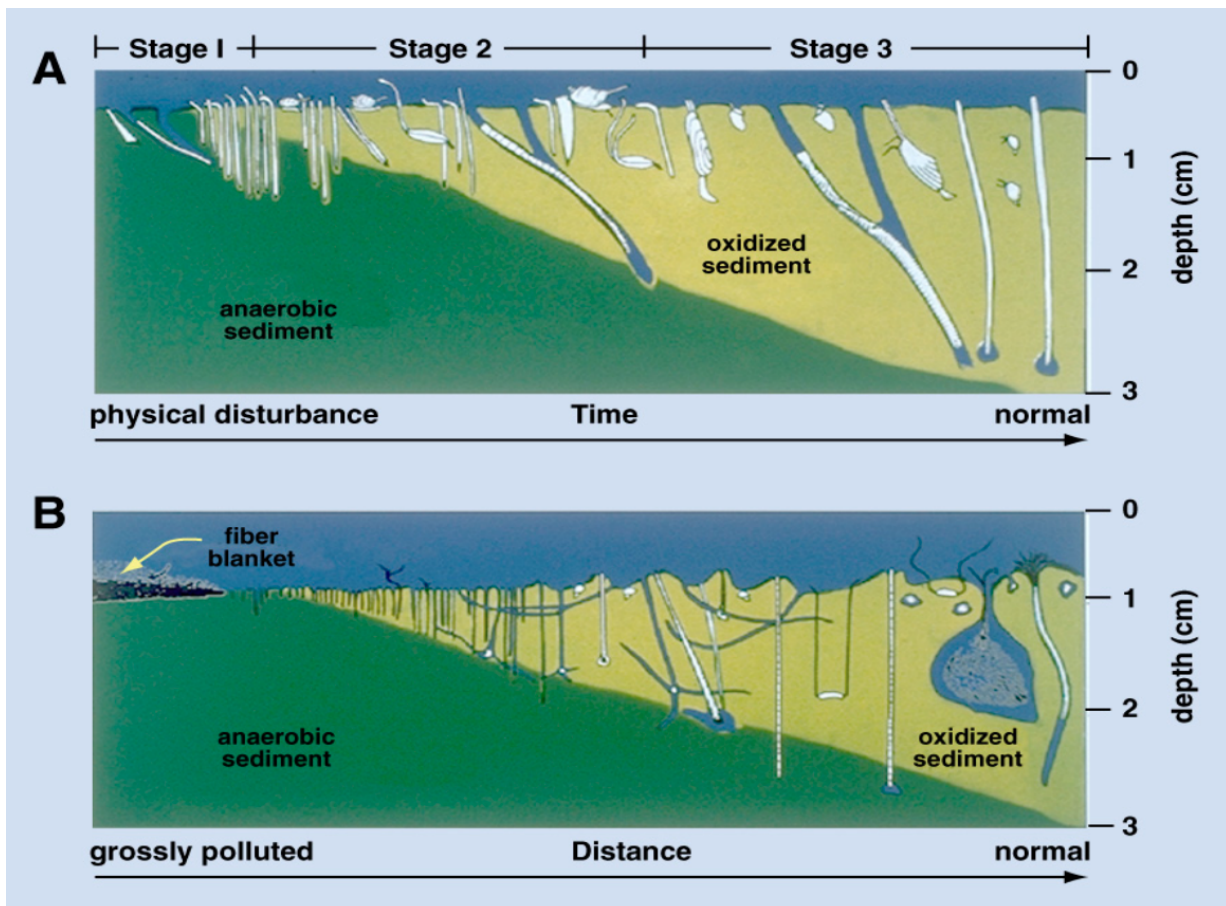


Figure 2. Soft-bottom benthic community response to (A) physical disturbance and (B) organic enrichment (from Rhoads & Germano 1982).

Although there are many imaged structures or features that can be measured from SPI images depending on the objectives of a particular SPI survey, there is a relatively short list of key parameters that are routinely measured and, as of 2017, required in the ASEA guidance for EBS SPI surveys in Mexican waters. These parameters include:

- Sediment type (grain size major mode and range)
- Depositional layers (e.g., drilling muds)
- Prism penetration depth
- Boundary roughness
- Apparent redox potential discontinuity (aRPD) depth
- Evidence of organic enrichment (i.e., sedimentary methane, sulfur-oxidizing bacteria)
- Biological mixing depths (depth and type of observed biological structures, i.e., feeding pockets, burrows, and organisms)
- Infaunal successional stage (inferred from types of animal-sediment relationships observed in each image as described in Rhoads and Germano 1982).

Figure 3 shows two SPI images from a dredging and capping project conducted near Juneau, Alaska, in early 2019. The key features listed above that were observed in these images are labeled. Note that these images show disposed anthropogenic deposits, a sand cap over a dredged material layer on the left, and disposed dredged material layer on the right. Any anthropogenic deposit that contrasts in color or texture with the ambient bottom can be detected and measured with SPI—this includes drilling muds and cuttings (Maxon, 2019; DBTWG 2011). How the labeled features are measured manually and how we are now automating those measurements in the iSPI image processing platform, developed by Maxon, is discussed and illustrated in the sections that follow.

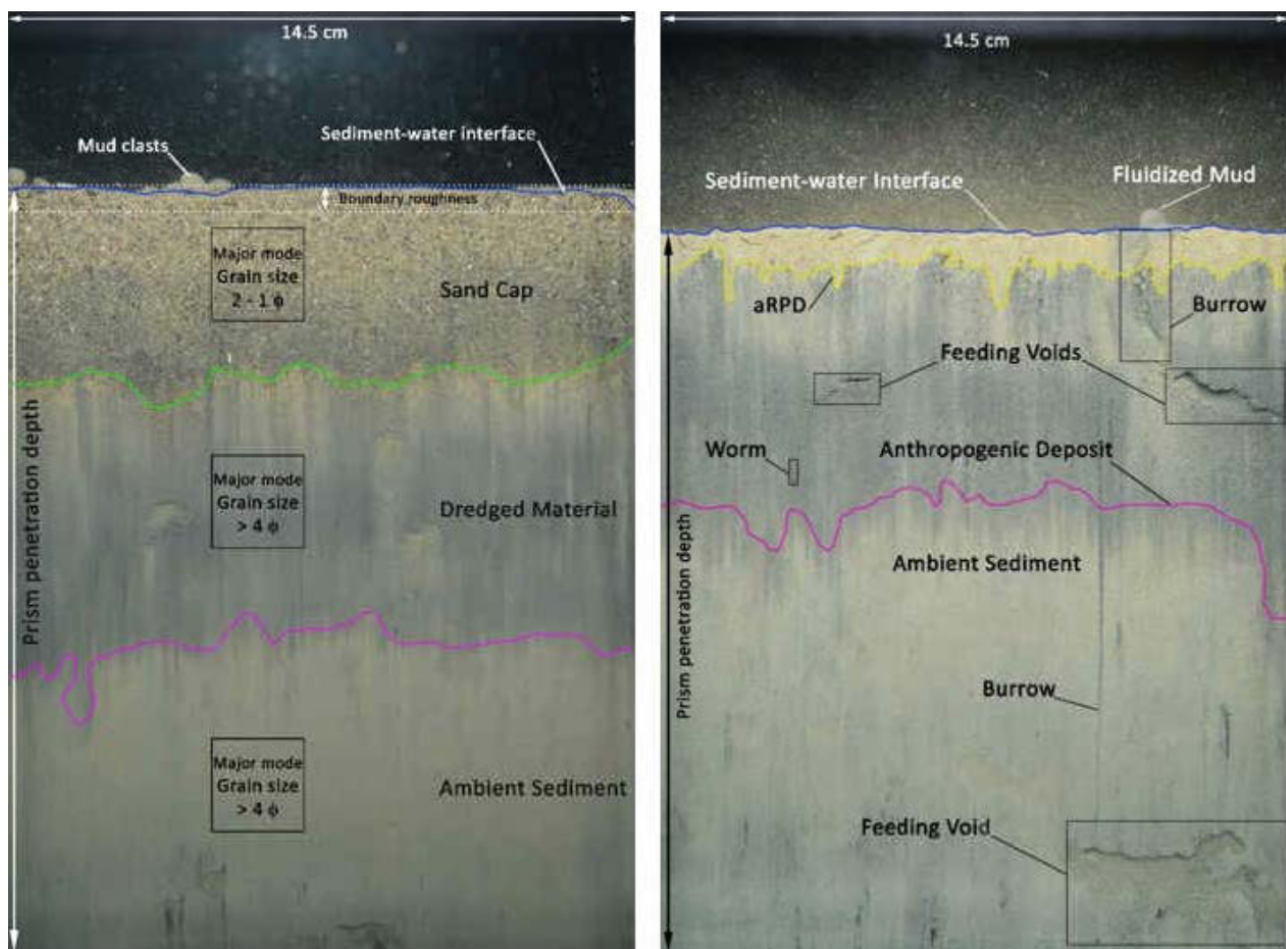


Figure 3. Physical features (left) and biological features (right) observed and measured in SPI images. These features were manually drawn and labeled by an image analyst. Scale: image width = 14.5 cm.

iSPI Image Analysis Platform

In 2020, Maxon designed a MATLAB®-based SPI/PV2 image processing platform (iSPI v0.1a) that integrates image files and field-collected metadata, stored in Microsoft® Excel spreadsheets, and provides image analysts with a custom graphical user interface (GUI) that guides them through the process of measuring and/or adding descriptive comments for key imaged features (Figure 4).² Data are stored in the system for review, revised if needed, and undergo quality assurance (QA) verification by a senior SPI scientist. Following the QA review of all measured and descriptive parameters, SPI/PV data can be easily exported, compiled, and used to generate the data products described in this report.

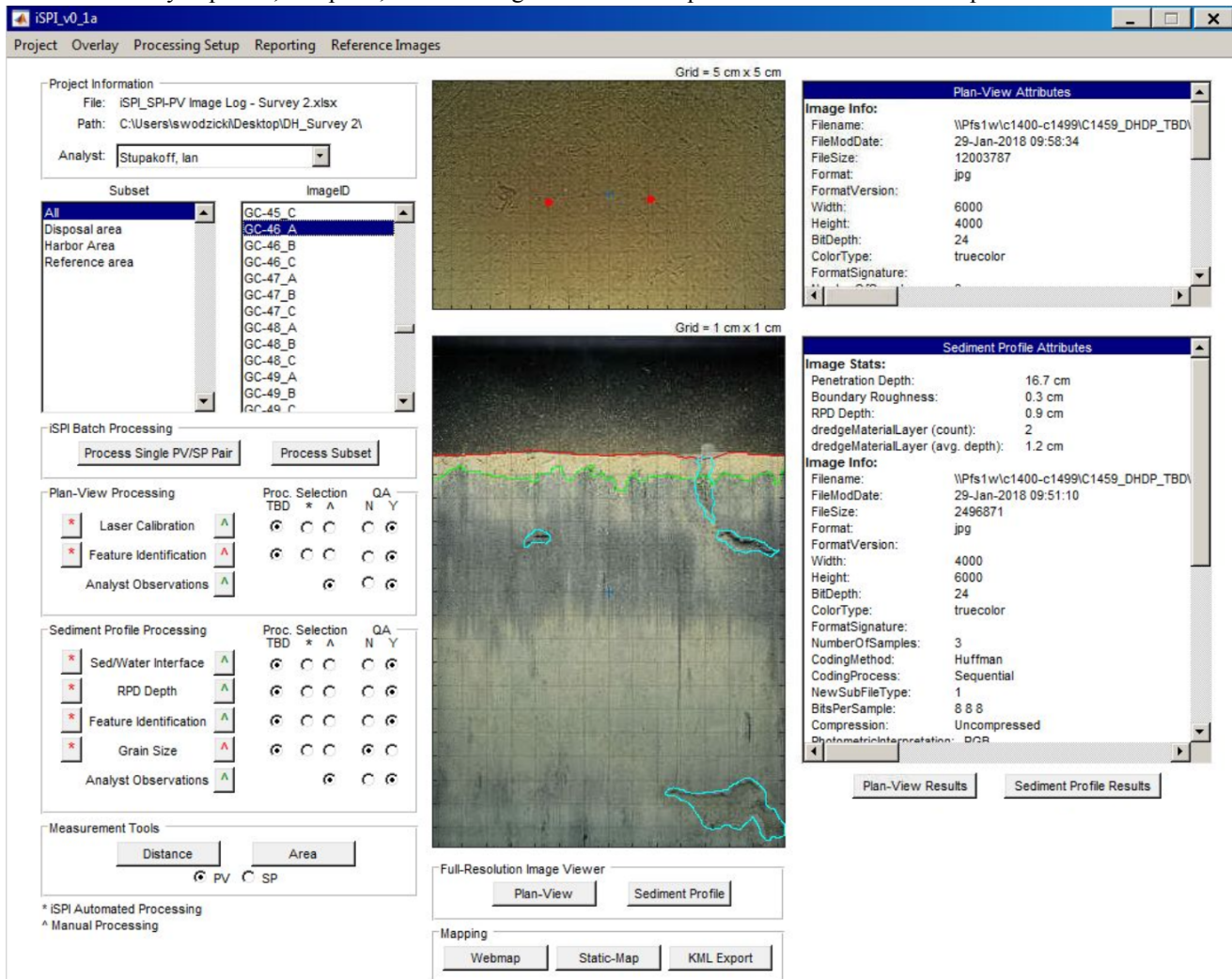


Figure 4. The iSPI user interface. The analyst can measure features manually or turn on the automated measurement algorithms. Data is stored for QA review by a second analyst. The attributes box lists the measurements being made in real-time.

The subsection that follows describes how each key SPI parameter is measured manually by the image analyst in iSPI and summarizes the underlying interpretative rationale for each parameter.

Manual Image Analysis in iSPI

² The iSPI platform is designed to handle collocated plan view images also. This paper is focused on the SPI analyses only, but automation of the key plan view image measurements is also under development.

Sediment Type

Sediment grain size major mode and range are estimated visually by comparing the texture in each image with a photograph set (grain size comparators) that was generated by imaging a series of sieved Udden-Wentworth sediment size class samples (equal to or less than coarse silt up to granules) placed against the SPI camera prism in the laboratory. Seven grain size classes (in phi units) are on this comparator: >4 (silt-clay), 4 to 3 (very fine sand), 3 to 2 (fine sand), 2 to 1 (medium sand), 1 to 0 (coarse sand), 0 to -1 (very coarse sand), and <-1 (granule and larger). The lower limit of optical resolution of the photographic system is about 62 microns, allowing recognition of grain sizes equal to or greater than coarse silt (>4). The image analyst typically records the major mode (predominant grain size across the entire image) and total grain size range (minimum to maximum particle size) observed in each image in iSPI. If distinct strata are evident as in the left image in Figure 3), then the analyst may manually document the major modal grain size for each layer.

Prism Penetration Depth

The SPI prism penetration depth is the average depth, in centimeters, from the SWI to the bottom of the image (Figure 3). The penetration depth is a function of the bearing capacity and shear strength of the sediments as well as certain camera frame settings (number of weights added, prism stop collar height). If these are fixed during a survey, then the relative penetration values from locations with comparable grain sizes provide a measure of the relative water content of surface sediments. Seasonal changes in camera prism penetration have been observed in some studies and are related to the control of sediment geotechnical properties by bioturbation (Rhoads and Boyer 1982). Consolidated or relic clayey sediments, and well-sorted and shell-containing sands, can be difficult to penetrate even with a fully weighted camera system.

To measure the penetration depth, the analyst carefully traces the SWI in each image (Figure 3) and iSPI calculates the total cross-sectional area of the sediment column in the image. This area is then divided by the linear width (14.5 cm) of the image to determine the average penetration depth that is displayed on the iSPI GUI (Figure 4) in real time.

Surface Boundary Roughness

Once the SWI is traced, iSPI determines the surface boundary roughness (Figure 3) automatically by calculating the vertical distance, in centimeters, between the highest and lowest points of the SWI. The surface boundary roughness may be related to either physical (e.g., rippled sands) or biological processes (e.g., burrow openings, fecal mounds, foraging depressions); the inferred origin of the boundary roughness is manually noted by the analyst in iSPI.

Thickness of Depositional Layers

A key capability of SPI technology is its ability to capture undisturbed views of depositional layers, either natural or anthropogenic, deposited on the seafloor. Any layer (down to the millimeter scale and up to about 20 cm—the height of the SPI prism window) that contrasts in color and/or texture with the ambient sediments, such that contact point between the layers is visible in the images, can be measured. This allows the spread or distribution of any anthropogenic sea bed deposit, such as drill muds or cuttings around an exploratory well, to be very accurately mapped.

During image analysis, the bottom of each depositional layer present is traced by the analyst, and iSPI automatically calculates the average thickness relative to the SWI or any other datum specified by the analyst.

Apparent Redox Potential Discontinuity Depth

Near-surface marine sediments are typically aerobic and have higher optical reflectance than the underlying reduced or anaerobic sediments. These differences in reflectance with depth in the sediment column are readily apparent in SPI images (Figure 3). The oxidized surface sediment particles are coated with ferric hydroxide, which has brownish or olive color, while reduced sediments below this oxygenated layer are darker, generally gray to black (Fenchel 1969; Lyle 1983). The boundary between the colored ferric hydroxide surface sediment and underlying gray to black sediment is called the apparent redox potential discontinuity (aRPD). Note that this measurement is referred to as the apparent RPD as the actual RPD is the horizon that separates the positive oxidation/reduction potential (Eh) (oxidizing) region of the sediment column from the underlying negative Eh (reducing) region, which can only be determined with microelectrodes.

Changes in the aRPD depths can be detected over days to months depending on the nature of the environmental setting and the benthic disturbance. Figure 2 is a schematic of the typical response of a soft-bottom benthic system to a major benthic disturbance. The deepening of the aRPD over time following the disturbance is a function of the rate at which both adult and larval infaunal recruitment occurs; this recruitment will depend on season and the areal extent of the disturbance. The aRPD is a key parameter for documenting changes (or gradients) that develop over time in response to benthic disturbance factors, such as natural or anthropogenic depositional events, as well as temporal (seasonal or yearly cycles) changes in environmental factors, such as water temperature, organic loading, and seasonal infaunal recruitment. Overall, time-series aRPD measurements following a disturbance are a diagnostic element in assessing the rate and degree of recovery in an area following a perturbation (Rhoads and Germano 1982, 1986).

The average aRPD depth is measured in each image by the analyst manually tracing the color transition redox boundary across the image. This boundary can be undulated or wavy as a function of the distribution of individual macrofauna and their localized biogenic mixing activities. The average depth of the aRPD is calculated in iSPI by subtracting the aRPD boundary depth from the SWI. The visual detection of the aRPD requires the optical contrast between oxidized and reduced finer-grained particles. It is often difficult to determine the depth of the aRPD in well-sorted sands that have little to no silt or organic matter in them.

Organic Loading, Sedimentary Methane, and Thiophilic Bacterial Colonies

If organic loading is high in marine sediments, then porewater sulfate is depleted and methanogenesis occurs. In SPI images, methanogenesis can be revealed by the appearance of methane bubbles in the sediment column. These gas-filled voids are readily discernible in SPI images because of their irregular shape and glassy texture (due to the reflection of the strobe off the gas). A potentially related feature that indicates an area is suffering severe sediment oxygen demand due to organic enrichment and/or depleted water column dissolved oxygen levels (i.e., hypoxia or anoxia) is the presence of the sulfur-oxidizing bacterial colonies at or just below the SWI. These bacterial colonies have diagnostic bright white or orange filamentous morphology that has been documented in numerous SPI surveys (Germano et al. 2011). The presence of sulfur-oxidizing bacterial colonies appear when boundary-layer dissolved oxygen concentrations drop into the “hypoxic” range between 0–1 mL/L (Rosenberg and Diaz 1993).

During image analysis, if the image analyst notes the presence of methane voids, each void can be traced and labeled and iSPI can then count the voids and determine the total area occupied by sedimentary methane in the image. If sulfur-oxidizing bacterial colonies are evident in the images, either at the SWI or at depth, the analyst notes the presence in the comment field in iSPI.

Biological Mixing Depth

The depth to which sediments are bioturbated, or the biological mixing depth, can be an important parameter for understanding and accurately modeling nutrient or contaminant flux in sediments. Bioturbation models typically include a near-surface layer where both porewater and sediment particles are thoroughly mixed by benthic infauna in an approximately random process as a function of organism density and their structures (e.g., see Francois et al. 2002). Some have used the vertical color change or aRPD depth measured in SPI images to define this upper, thoroughly mixed biologically active zone (Clarke et al. 2001; Solan et al. 2004). While the aRPD is a potential measure of biological mixing depth, evidence of biological activity (burrows, voids, or the actual animals) is often seen well below the aRPD depth. Biogenic mixing still occurs in these deeper sediments, but it is mostly controlled by non-random or local particle transport by larger organisms, their biogenic structures (e.g., tube gallery as described in Francois et al. 2002), and/or their activities, such as head-down deposit feeding (Diaz and ARCADIS 2008). These deeper, but more localized, biological mixing depths can be estimated in SPI images by measuring the maximum depths observed of imaged feeding voids, burrows, or the organisms themselves in the sediment column (Germano & Associates 2004).

To estimate the deeper biological mixing depths in SPI images, the analyst identifies and traces the organisms, feeding voids, and burrows observed in the SPI image. The depth to the bottom of the deepest of these features is considered the maximum biological mixing depth. The average depth of the features can also be calculated.

Infaunal Successional Stage

Identification of successional stages in SPI images is based on the theory that organism-sediment interactions in fine-grained sediments follow a predictable sequence after a major disturbance. This theory (first presented in Pearson and Rosenberg [1978] and further developed for interpretation of SPI images in Rhoads and Germano [1982]) is based on the concept that primary succession results in “the predictable appearance of macrobenthic invertebrates belonging to specific functional types following a benthic disturbance. These invertebrates interact with sediment in specific ways. Because functional types are the biological units of interest...the definition does not demand a sequential appearance of particular invertebrate species or genera” (Rhoads and Boyer 1982).

This continuum of change in marine, soft-bottom, infaunal communities after a disturbance has been divided into four primary stages (Stages 1 through 3 are generalized and illustrated in Figure 2):

- Stage 0, indicative of a sediment column that is largely devoid of macrofauna, occurs immediately following a major physical disturbance or in close proximity to an organic enrichment source.
- Stage 1 is the initial community of tiny, densely populated, tubicolous, surface-dwelling polychaete assemblages.
- Stage 2 is the start of the transition to head-down deposit feeders and can also consist of shallow-dwelling bivalves and tube-dwelling amphipods.
- Stage 3 is the mature, equilibrium community of deep-dwelling, head-down deposit feeders that create distinctive feeding voids and aerated burrows that are visible in SPI images.

In temporal and spatially dynamic marine environments, benthic communities are unlikely to progress completely and sequentially through all four stages in accordance with the idealized conceptual model depicted in Figure 2. Various and transitional combinations of these basic successional stages are possible (e.g., Stage 1 going to Stage 2). More frequently, secondary succession can occur in response to additional labile carbon input to surface sediments, with surface-dwelling Stage 1 or 2 organisms co-existing at the same time and place with Stage 3, resulting in the assignment of a “Stage 1 on 3” or “Stage 2 on 3” designation.

As a final note, the successional dynamics of benthic invertebrate communities noted above are based on well-documented studies of fine-grained benthic environments; the successional dynamics of invertebrate communities in sand and coarser sediments are less well-known, and the interpretation of successional patterns from SPI images in sandy and coarse-grained bottoms is relatively limited.

Based on the biota, animal-sediment relationships, and the presence of biogenic structures (e.g., feeding voids), the image analyst assigns an infaunal successional stage to each image during analysis.

Automated Image Analysis in iSPI

With the exception of the infaunal successional stage, all of the key parameters measured from SPI images are visually discernible combinations of textures, colors, and linear or areal shapes. Past efforts to automate the SPI image analysis process achieved limited success (Ghita et al. 2003, 2004; Romero-Ramirez et al. 2013). These two attempts used a combination of automatic and semiautomatic image processing techniques to make measurements of linear features such as the SWI and aRPD, as well as polygons to characterize features such as feeding voids. Neither effort attempted to estimate grain size textures. Independently, the U.S. Geological Survey developed a statistical method to extract estimates of grain size particle distributions from images using a transferable wavelet method (Buscombe 2013). We investigated the use of this method on examples from our SPI image library and found the particle size distributions generated were biased high relative to our visual grain size major modal estimates.

In the last year, Maxon has developed and tested several algorithms for automating the measurement of SPI features. All of target parameters can be measured with one of three approaches as shown in Table 1.

Table 1. Computer Vision Approaches for Automating the Measurement of SPI Features

Approach(es)	Parameters Measured	Current Status
Segmentation-based Fractal Texture Analysis (SFTA) → Convolutional Neural Network (CNN for Image Classification)	Grain size	SFTA prototype in use; currently using SFTA to develop an expanded set of labeled images that can be used to train a CNN-based classifier.
Windowed Gradient Analysis for Interface Delineation	Sediment-water interface - Penetration depth - Boundary roughness Depositional layers aRPD depth	Prototype algorithm in use
Convolutional Neural Network (CNN for Object Detection/Localization and/or Semantic Segmentation)	Organisms Feeding structures Burrows Methane Sulphur-oxidizing bacteria	Training image libraries under construction; prototype CNN-based object detectors to be completed in May 2018.
Convolutional Neural Network (CNN for Image Classification)	Infaunal successional stage	Not planned currently, but may be possible if adequate training data are available.

Grain Size

The algorithm used to automatically identify major modal grain size (phi units) in the SPI images is currently based on a Segmentation-based Fractal Texture Analysis (SFTA) approach (Costa et al. 2012). The approach uses a machine learning classifier to predict grain sizes in relatively small areas (thumbnails) of the image. The number of thumbnails can be preset or adjusted by the image analyst depending on the texture heterogeneity in an image set or individual image (Figure 5). The multiclass Naïve Bayes (NB) classifier model was trained using a library of 512x512-pixel thumbnail images with known phi size classes. The SFTA algorithm decomposes each thumbnail image into a series of black-and-white images using different thresholds. The black-and-white images are then used to define a feature vector that is related to the texture that one sees in the original image. The feature vector is fed into NB classifier to get the final grain size determination. This automated approach produces a grain size major mode estimate for each subarea of the image.

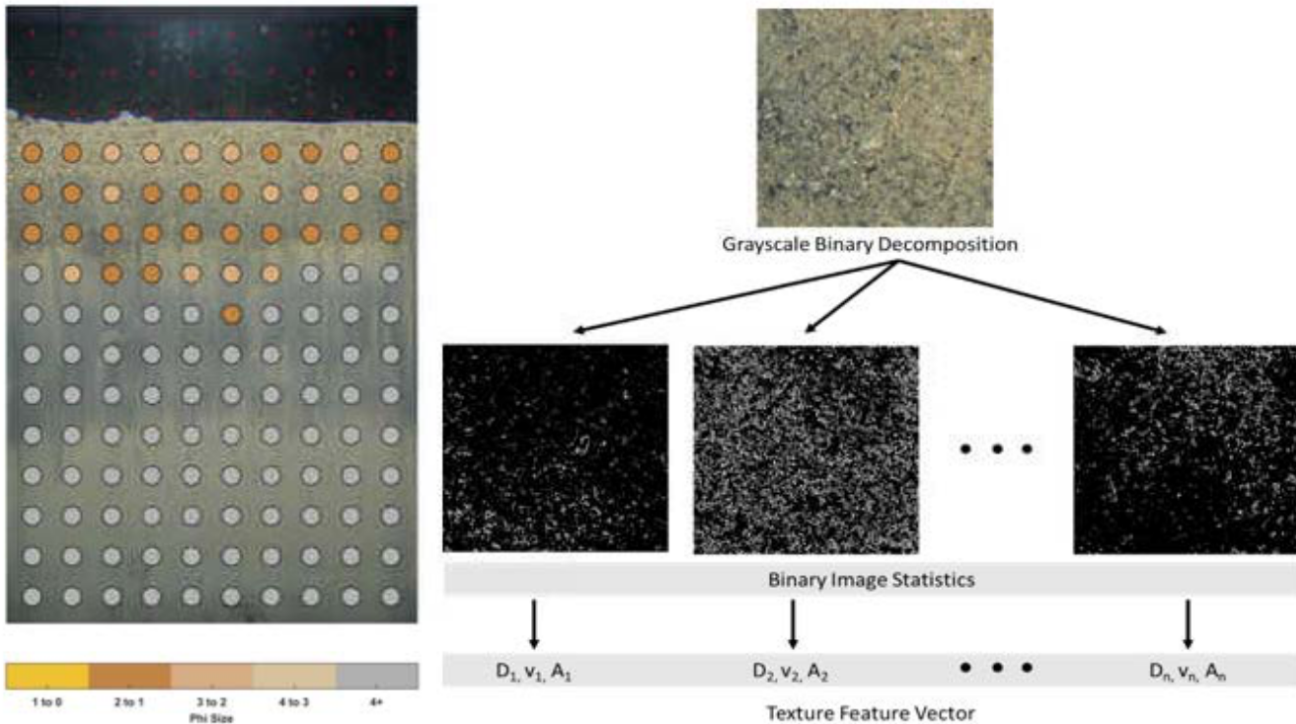


Figure 5. SFTA grain size determinations on a fixed (10 x 15) prediction grid (left). Schematic of SFTA texture algorithm (right).

While the performance of the SFTA approach is acceptable, there is room for improvement. Moving forward we will be using the SFTA results to augment and streamline our efforts to develop an expanded set of labeled images that can be used to train more advanced machine learning classifiers. For example, using our current SFTA-based estimates of grain size, QA'd to correct for any misclassifications, we can quickly and cost-effectively generate a large set of training images that can be used to train a convolutional neural network (CNN)-based classifier to predict grain size. We anticipate that a CNN-based classifier will yield superior performance when compared to our current SFTA-based approach (see additional discussion of CNNs in the following subsection on biogenic feature detection).

Interface Delineation

The algorithm developed to identify/characterize the SWI is based on a localized gradient analysis within an analysis window that moves across the image. In this context, an interface is considered to be a multipoint linear feature that spans the entire horizontal extent of an image, separating two regions of consistent color and/or texture. For example, the SWI is an interface that separates sediment bed from the overlying water column.

Similar to what is done to define the SWI, the same approach and algorithm implementation is leveraged to identify/characterize depositional layers, the aRPD, and other interfaces such as boundaries between sand over mud strata (Figure 6). As illustrated in Figure 6, the uncertainty at any point along the interface being defined is indicated so that the supervising analyst can edit or correct if needed. The iSPI GUI also shows the calculated interface depth, relative to the SWI, so the analyst can evaluate results in real time.

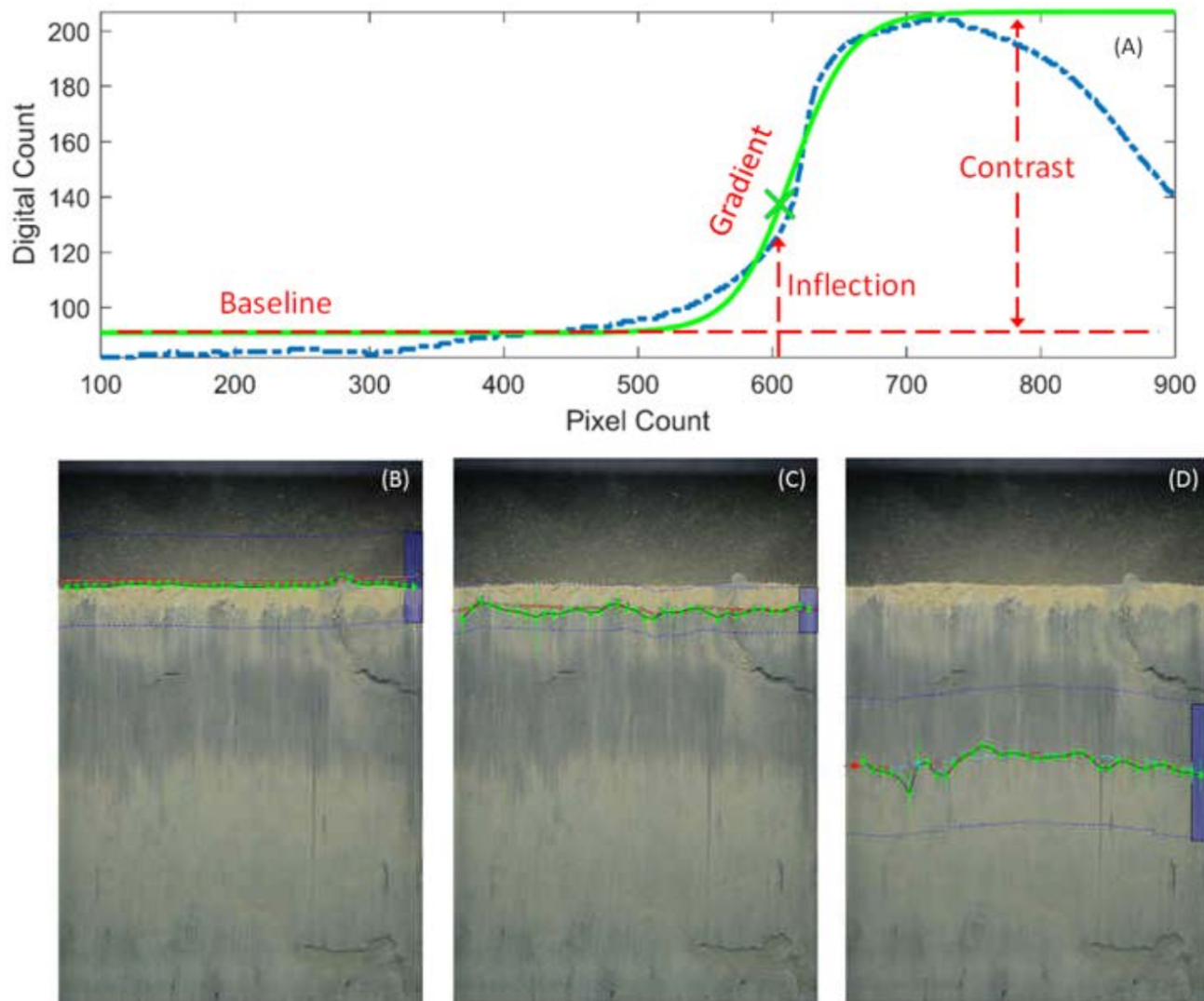


Figure 6. Gradients and interfaces between adjacent layers are characterized using average grayscale values in adjustable-sized analysis windows that are fit using a 4-parameter logistic curve (A). Analysis windows slide across the image allowing iSPI to draw the interface across the entire image (B–D). Uncertainty associated with the 4 logistic parameters that are estimated are used for QA to help the analyst evaluate real-time algorithm performance.

Biogenic Feature Detection Using Convolutional Neural Networks

Accurate and automatic detection and localization of objects in SPI images (e.g., infauna, feeding structures, methane bubbles, etc.) is challenging. However, over the last 5 to 10 years, extensive and rapid progress has been on a wide variety of image classification and object detection problems using deep learning and convolutional neural networks. In some cases, the performance of CNN-based object detectors has approached—and even exceeded—what humans are able to achieve.

Two challenges that must be addressed to effectively use a CNN-based approach for object detection are:

1. Large sets of labeled images must be developed for training and validation.
2. Optimized hardware and software must be utilized to ensure that a deep CNN can be trained effectively and in a reasonable amount of time (workstations and/or cloud computing resources with graphics processing unit-accelerated computing capabilities are required).

Over the next year, Maxon will continue developing large sets of labeled SPI images to advance and refine CNN-based object detectors and to evaluate new neural network architectures as they emerge from the computer vision research community. Labels and annotations will be added to images using a combination of iSPI, custom in-house image annotation software, and MATLAB's® Image Labeler application (Figure 7). While the time and effort needed to develop these sets of labeled images is substantial, we are confident that our diverse image library and our unique combination of staff expertise and onsite computing resources will make the investment worthwhile and move us closer to a fully automated SPI processing system.

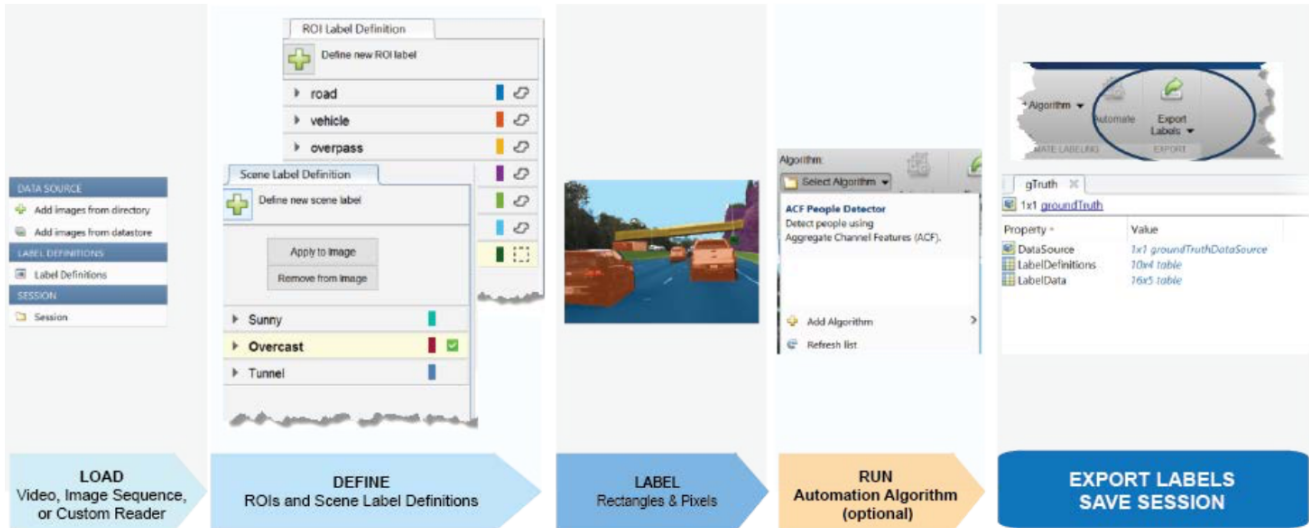


Figure 7. The MATLAB® Image Labeler application provides an easy way to label rectangular regions of interest (ROIs) for object detection, pixels for semantic segmentation, and scenes for image classification.

Discussion

Recent advances in computer image processing techniques allow SPI images to be analyzed effectively in a supervised automated fashion. Standardization of and transparency in the SPI data generation process may foster the increased use and regulatory acceptance of this effective and well-established seafloor survey technology. In the coming months, Maxon's iSPI software should be able to semiautomatically measure all of the key SPI parameters discussed above with the exception of the infaunal successional stage designation. Successional stage is a semiqualitative designation and it can be dependent on the experience of the image analyst. If the automatic detection and localization of objects, such as subsurface feeding voids, can be optimized, then the density and depth of such features may be readily mapped and some combination of specific mapped metrics, rather than the analyst-inferred successional stages, may be used to delineate benthic ecological disturbance gradients.

Germano et al. (2011) point out that the interpretation of the sedimentological and ecological significance of variations in sediment colors, textures, and patterns observed in SPI images requires an in-depth scientific understanding of geological, geochemical, and biological benthic processes. There will always be a need for skilled and experienced SPI scientists to evaluate and interpret SPI image data sets. The objective of this ongoing work is to streamline and standardize the extraction of the main suite of SPI parameters from the images using state-of-the-art computing image processing and deep learning technologies. These approaches can be applied to plan view and video seafloor imagery also. It is hoped that these advances will allow SPI image data sets to be rapidly generated immediately following, and ultimately perhaps even during, image acquisition. These data sets will be standardized, transparent, and easily stored and managed in project databases in support of environmental assessments for the offshore energy industry.

Acknowledgments

We would like to thank the U.S. Department of Energy's Office of Energy Efficiency & Renewable Energy for providing funding under Contract DE-FE0004537 to design, develop, and test the automated image analysis algorithms discussed here.

References

- Buscombe, D. 2013. Transferable wavelet method for grain-size distribution from images of sediment surface and thin sections, and other natural granular patterns. *Sedimentology* 60:1709–1732.
- Clarke, D.G., M.R. Palermo, and T.C. Sturgis. 2001. Subaqueous cap design: Selection of bioturbation profiles, depths, and rates. DOER Technical Notes Collection (ERDC TN-DOER-C21). U.S. Army Engineer Research and Development Center, Vicksburg, MS.
- Costa, A.F., G. Humpire-Mamani, and A.J.M. Traina. 2012. An efficient algorithm for fractal analysis of textures. pp. 39-46. In Graphics, Patterns and Images (SIBGRAPI), 2012 25th SIBGRAPI Conference on. IEEE. August.
- CSA. 2006. Effects of oil and gas exploration and development at selected continental slope sites in the Gulf of Mexico, Volume II: Technical Report. OCS Study MMS 2006-045. U.S. Department of the Interior, Minerals Management Service, Gulf of Mexico OCS Region, New Orleans, LA. Continental Shelf Associates, Inc., Jupiter, FL.
- DBTWG. 2011. Mississippi Canyon 252 Incident NRDA Sampling Plan: Offshore and deepwater softbottom sediment and benthic community structure survey. Deepwater Benthic Communities Technical Working Group. April 6.
- Despande, A. 2016. A beginner's guide to understanding convolutional neural networks.
<https://adeshpande3.github.io/adeshpande3.github.io/A-Beginner%27s-Guide-To-Understanding-Convolutional-Neural-Networks/>
- Diaz, R., and ARCADIS. 2008. Estimation of the biologically active zone, Newark Bay, New Jersey. R.J. Diaz and Daughters, Ware Neck, VA, and ARCADIS, Annapolis, MD. September.
- Diaz, R.J., G.R. Cutter, Jr., and D.M. Dauer. 2003. A comparison of two methods for estimating the status of benthic habitat quality in the Virginia Chesapeake Bay. *Journal of Experimental Marine Biology and Ecology* 285:371–381.
- Diaz, R.J., G.R. Cutter, Jr., and C.H. Hobbs. 2004. Potential impacts of sand mining offshore of Maryland and Delaware: Part 2—Biological considerations. *Journal of Coastal Research* 20:61–69.
- Diaz, R.J., L.J. Hansson, R. Rosenberg, P.C. Gapcynski, and M.A. Unger. 1993. Rapid sedimentological and biological assessment of hydrocarbon contaminated sediments. *Water, Air, and Soil Pollution* 66:251–266.
- Fenchel, T. 1969. The ecology of marine macrobenthos IV. Structure and function of the benthic ecosystem, its chemical and physical factors, and the microfauna communities with special reference to the ciliated protozoa. *Ophelia* 6:1–182.
- Francois, F., M. Gerino, G. Stora, J. Durbec, and J. Poggiale. 2002. Functional approach to sediment reworking by gallery-forming macrobenthic organisms: Modeling and application with the polychaete *Nereis diversicolor*. *Mar. Ecol. Prog. Ser.* 229:127–136.
- Germano & Associates. 2004. Benthic macrofaunal activity at Hunters Point, San Francisco Bay. Germano & Associates, Bellevue, WA.

- Germano & Associates. 2010. Evaluation of sediment and benthos characteristics at the completed northern pipeline route for the Neptune deepwater port location in Massachusetts Bay, USA: First post-construction survey. Prepared for Ecology & Environment, Inc. Germano & Associates, Bellevue, WA.
- Germano, J.D., D.C. Rhoads, R.M. Valente, D.A. Carey, and M. Solan. 2011. The use of sediment profile imaging (SPI) for environmental impact assessments and monitoring studies: Lessons learned from the past four decades. *Oceanogr. Mar. Biol. Ann. Rev.* 49:235–298.
- Ghita, O., P.F. Whelan, and R. Kennedy. 2003. A practical approach for analysing SPI images. *SCI 2003 - Systemics, Cybernetics and Informatics*: 141–146 (July), Florida, USA.
- Ghita, O., P.F. Whelan, and R. Kennedy. 2004. The application of image processing algorithms to the analysis of SPI images. Sediment Profile Imagery Colloquium of Experts (SPICE), NUI, Galway, April 5–7.
- Lyle, M. 1983. The brown-green colour transition in marine sediments: A marker of the Fe(III)-Fe(II) redox boundary. *Limnol. Oceanogr.* 28:1026–1033.
- Pearson, T.H., and R. Rosenberg. 1978. Macrofaunal succession in relation to organic enrichment and pollution of the marine environment. *Oceanogr. Mar. Biol. Ann. Rev.* 16:229–311.
- Rhoads, D.C., and L.F. Boyer. 1982. The effects of marine benthos on physical properties of sediments, pp. 3–52. In: *Animal-Sediment Relations*. P.L. McCall and M.J.S. Tevesz (eds). Plenum Press, New York, NY.
- Rhoads, D.C., and S. Cande. 1971. Sediment profile camera for *in situ* study of organism-sediment relations. *Limnology and Oceanography* 16:110–114.
- Rhoads, D.C., and J.D. Germano. 1982. Characterization of benthic processes using sediment profile imaging: An efficient method of remote ecological monitoring of the seafloor (REMOTSTM System). *Mar. Ecol. Prog. Ser.* 8:115–128.
- Rhoads, D.C., and J.D. Germano. 1986. Interpreting long-term changes in benthic community structure: A new protocol. *Hydrobiologia* 142:291–308.
- Rumohr, H., and H. Schomann. 1992. REMOTS sediment profiles around an exploratory drilling rig in the southern North Sea. *Mar. Ecol. Prog. Ser.* 91:303–311.
- Romero-Ramirez, A., A. Grémare, M. Desmalades, J.C. and Duchêne. 2013. Semi-automatic analysis and interpretation of sediment profile images. *Env. Modelling & Software* 47:42–54.
- Rosenberg, R., and R.J. Diaz. 1993. Sulfur bacteria (*Beggiatoa* spp.) mats indicate hypoxic conditions in the inner Stockholm Archipelago. *Ambio* 22:32–36.
- Solan, M., B.J. Cardinale, A.L. Downing, K.A. Engelhardt, J.L. Ruesink, and D.S. Srivastava. 2004. Extinction and ecosystem function in the marine benthos. *Science* 306:1177–1180.
- Valente, R.M., D.C. Rhoads, J.D. Germano, and V.J. Cabelli. 1992. Mapping of benthic enrichment patterns in Narragansett Bay, Rhode Island. *Estuaries* 15:1–17.